Journal of
Chemical Engineering & Process Technology

El-Shamy et al., J Chem Eng Process Technol 2016, 7:1
DOI: 10.4172/2157-7048.1000273

Research Article
Open Access

Mitigation of Sulfide Attach on α -Brass Surface by Using Sodium (Z)-4-Oxo-4-p-Tolyl-2-Butenoate

El-Shamy AM[1]*, Amal MA Elkarim[1] and Atef Kalmouch[2]

[1]*Physical Chemistry Department, Electrochemistry and Corrosion Lab, National Research Centre, El-Bohouth St. 33, Dokki, PO 12622, Giza, Egypt*
[2]*Peptide Chemistry Department, National Research Centre, El-Bohouth St. 33, Dokki, PO 12622, Giza, Egypt*

Abstract

The corrosion inhibition efficiency of α-brass was evaluated in unpolluted and sulfide polluted 3.5% NaCl. The Sodium (Z)-4-Oxo-4-p-Tolyl-2-Butenoate (SOTB) has been used as safe organic corrosion inhibitor instead of benzotriazole. The electrochemical methods were used to monitor the effect of inhibitor on corrosion inhibition of brass. The results showed that this inhibitor act as cathodic and anodic inhibitor for the surface of brass in both chloride and sulfide polluted medium. Brass electrodes were subjected to characterization by SEM and EDS to prove the probable mechanism. The inhibition efficiency and the persistence of protective film are depends on the inhibitor concentration in both chloride and sulfide media.

Keywords: Corrosion; Corrosion inhibition; α-brass; SOTB; Sulfide attack; Mechanisms

Introduction

Inhibition of sulfide attack on brass surface is considered as the most important tasks in industrial applications. It is well known that copper and its alloys are relatively noble but it is easily affected by the rich oxygen environments [1-10]. The surface deterioration of brass structures are depending on the dezincification process. The corrosion process of brass is depending on the chloride and sulfide concentration. It is well known that the organic compounds are commonly used to protect the brass in corrosive environment [10-17]. In chloride content solution the benzotriazole is considered the most common, effective corrosion inhibitor specifically for copper and as well as its alloys. In case of polluted sulfide solution the benzotriazole losses its effect due to failure of the formed protective film. Till the present there is no way to get rid sulfide attack on the surface of copper and its alloys. The research is interested in how to decrease the effect of sulfide attack via improvement the stability of protective film. There are many industries; the brass is included in e.g., refrigeration [18,19], desalination [20], petrochemical industries [21,22]. The involved mechanism of corrosion (brass and environment) and inhibition process (brass and inhibitor) are studied in many papers [23-39].

The explaining of the proposed inhibition efficiency is concerned with studying the physical or chemical meaning of the interaction between inhibitor and the metal surface and as well as the environment. The high inhibiting efficiency of SOTB could be explained by these proposed mechanisms. The first proposed mechanism is concerned with the protective film formation on the brass surface in chloride medium. The following equations illustrate the proposed reactions of brass in unpolluted sulfide media [35-39].

$$CuZn=Cu^{o}+Zn^{2+}+2e^{-} \quad (1)$$

$$Cu^{o}=Cu^{2+}+2e^{-} \quad (2)$$

$$Cu+2Cl^{-}=CuCl_2^{-}+e^{-} \quad (3)$$

$$Zn^{o}=Zn^{2+}+2e^{-} \quad (4)$$

$$Zn+2Cl^{-}=ZnCl_2+2e^{-} \quad (5)$$

Equation 6 and 7 show the first proposed mechanism which attributed with the formation of protective film from the corrosion inhibitor which prevent the metal dissolution.

$$Cu^{+(aq)}+SOTB_{(aq)}=Cu\ (I)OTB_{(s)}+Na^{+}_{(aq)} \quad (6)$$

$$Zn^{+(aq)}+SOTB_{(aq)}=Zn\ (I)OTB_{(s)}+Na^{+}_{(aq)} \quad (7)$$

Figure 1 shows the adsorption of corrosion inhibitor SOTP on the brass surface which descripts the other mechanism, see equations 8 and 9.

$$Cu_{(s)}+SOTB=Cu{:}OTB_{(ads)}+Na^{+}_{(aq)} \quad (8)$$

$$Zn_{(s)}+SOTB=Zn{:}OTB_{(ads)}+Na^{+}_{(aq)} \quad (9)$$

In the neutral solutions it is now widely recognized that the sulfide ions are existed in environments around the metal surface in the form of HS^{-} ions. The brass corrosion is promoted by sulfide ions by adsorption step see equations 10 and 11. The formed adsorbed layer could be oxidized to form CuS and ZnS, see Equations 12 and 13 [37-39].

$$HS^{-}+Cu=Cu{:}\ HS^{-} \quad (10)$$

$$HS^{-}+Zn=Zn{:}\ HS^{-} \quad (11)$$

$$Cu{:}\ HS^{-}=CuS+H^{+}+2e^{-} \quad (12)$$

$$Zn{:}\ HS^{-}=ZnS+H^{+}+2e^{-} \quad (13)$$

The organic compound SOTB is not only used as corrosion inhibitor but also it has a biological effect. The amic acids gain their importance from being the precursors for the cyclic imides [40-43]. The amide moiety is an important constituent of many biologically active compounds. N-Phenyl- maleamic acids derivatives which contain amide moiety is known as selective herbicide antidotes [44]. Also in plant protection field, the maleamic acid has safener activity

***Corresponding author:** El-Shamy AM, Physical Chemistry Department, Electrochemistry and Corrosion Lab, National Research Centre, El-Bohouth St. 33, Dokki, PO 12622, Giza, Egypt, Tel: 00201222846136; E-mail: elshamy10@yahoo.com

Received January 14, 2016; **Accepted** February 07, 2016; **Published** February 13, 2016

Citation: El-Shamy AM, Elkarim MAA, Kalmouch A (2016) Mitigation of Sulfide Attach on α-Brass Surface by Using Sodium (Z)-4-Oxo-4-p-Tolyl-2-Butenoate. J Chem Eng Process Technol 7: 273. doi:10.4172/2157-7048.1000273

Citation: El-Shamy AM, Elkarim MAA, Kalmouch A (2016) Mitigation of Sulfide Attach on α-Brass Surface by Using Sodium (Z)-4-Oxo-4-p-Tolyl-2-Butenoate. J Chem Eng Process Technol 7: 273. doi:10.4172/2157-7048.1000273

for the plants where maleimides and isomaleimides are "prosafeners" and are converted in the plant tissue to the maleamic acid form, which is responsible for safening action [45]. In this paper the corrosion behavior of brass is monitored in uninhibited and inhibited chloride and sulfide medium. The present paper is aiming at how to try to mitigate the attack of sulfide ion on the brass surface.

Experimental

Materials

Electrode: Commercial brass is used as working electrode with a nominal composition of (Cu=67.22 and Zn=28.12). The electrode was in the dimensions of (1X1X0.2 cm). The brass electrodes were polished, washed, degreased in acetone and dried.

Electrolyte: 100 ml of 3.5% NaCl is used as unpolluted electrolyte and 0.01M sulfide ions S^{2-} were added as Na_2S.

Methods

Synthesis of the inhibitor: The organic solvents and the chemicals used in this paper were obtained from Sigma (USA) and Fluka (Switzerland) chemical companies; our corrosion inhibitor was subjected to full analysis using Infrared (IR) spectra, FT-IR Spectrum, Melting point, Elemental micro-analysis for carbon, hydrogen and nitrogen was measured. NMR spectra,(MS) and (TLC).

To a solution of (0.01 mol) maleic anhydride in (25 mL) of chloroform, a chloroform solution of (0.01 mol) p-toluidine was drop wisely added with stirring at room temperature when yellow precipitate is formed. Stirring was continued for two hours at room temperature then the resulted precipitate was filtered and dried to afford 95% yield, then purified by recrystallization from ethanol. m.p. 199.5-200.6°C; UV λ_{max}, Et.OH $_{nm}$ (log ε)=221.6 (4.189). IR (KBr): ν_{max}/cm^{-1} 3551-3435 (OH str), 3282 (NH str), 3100-2997 (CH=), 1810-1955 (mono substituted arom.), 1730-1635 (C=O), 1633-1600 (C=C), 1590-1540 (amide II bending), 1465-1400 (amide III str), 1399 (C=C arom), 1321-1220 (C-OH str), 865-800 (*p*-arom.), 860-660 (arom. ring system). ^{1}H NMR (500 MHz, (DMSO-d_6): δ=2.23 (s, 3H, CH_3), 6.27 (d, 1 H, CH=COOH), 6.41 (d, 1H, CH=CONH), 7.11 (d, 2H, o- arom.), 7.45 (d, 2H, m-arom), 10.34 (s, 1H, NH CO), 13.25 (s, 1H, COOH) ppm. MS (EI) m/z=205.07 [M^+]. Anal.: Calcd. For $C_{11}H_{11}NO_3$ (205.21): C (64.38), H (5.40), N (6.83) and O (23.39). Found: C (64. 26), H (5.33), N (6.82) and O (23.36). The inhibitor (Z)-4-Oxo-4-p-Tolyl-2-Butenoate was synthesized according to the scheme presented in Figure 2 and sodium carbonate was added drop wise to the inhibitor to form the sodium salt to make the inhibitor soluble in water.

Open circuit potential measurement: This method was used to monitor the open circuit potential (OCP) of brass electrode in certain immersion time in 3.5% NaCl. The experiment is carried out in the presence and absence of SOTB as a corrosion inhibitor and all measurements are registered till the steady state values were reached.

Potentiodynamic polarization measurements: The measurements of potentiodynamic polarization were carried out for brass electrode with an exposed area of 1 cm^2. The electrochemical cell is consisted of brass strip as working electrode, a platinum foil as counter electrode and a saturated calomel electrode (SCE) as reference electrode. The curves of potentiodynamic polarization were measured using a potentiostat/galvanostat (Autolab modules: PGSTAT302N) and the data obtained were analyzed using the NOVA software version 1.10. The brass strip was immersed in a 3.5% NaCl solution and allowed to reach steady state potential for period of time of about 30 min [46]. Each experiment was carried out in a 3.5% NaCl solution in the presence and absence of different concentrations of the SOTB. The scan rate was established at 1 mV/s and the inhibition efficiencies of the compounds were determined from corrosion currents using the Tafel extrapolation method.

Electrochemical impedance measurements: The electrochemical impedance measurements were estimated by using an AUTOLAB with frequency response analyzer (FRA), which included a potentiostat model PGSTAT302N. An AC sinusoid of ± 10 mV was applied at the corrosion potential (E_{corr}). The frequency range of 100 kHz-1 mHz was employed. The brass specimen with an exposing surface area of 1 cm^2 was used as the working electrode. A conventional three electrode electrochemical cell of volume of about 100 ml was used [47]. The values of polarization resistance (R_p) were also measured at different concentrations from sulfide ions and the corrosion inhibitor.

Surface characterization: The brass electrodes were characterized using SEM and the Energy Dispersive X-ray analysis (EDX) was used to identify the elemental analysis for the brass surface after polarization measurements.

Results and Discussion

Open circuit potential measurement

The values of open circuit potential of brass electrode at different concentration of SOTB are present in Figure 3. The results illustrated that the open circuit potentials are shifted towards more positive direction gradually from 25 till 250 ppm but in case of 300 ppm the potential shifted towards the more negative which prove that the 250 ppm is the recommended dose for the application use. The OCP values were -0.188, -0.184, -0.173 and -0.139 V for 25, 100, 150 and 250 ppm respectively but in case of 300 ppm of SOTB the potential shifted to more negative again with value of -0.221 V.

Potentiodynamic polarization curves

The effect of concentration of corrosion inhibitor was investigated by polarization curves and the results are resented in Figure 4a. It is clearly noticed that the effect of inhibitor, since the shift in cathodic

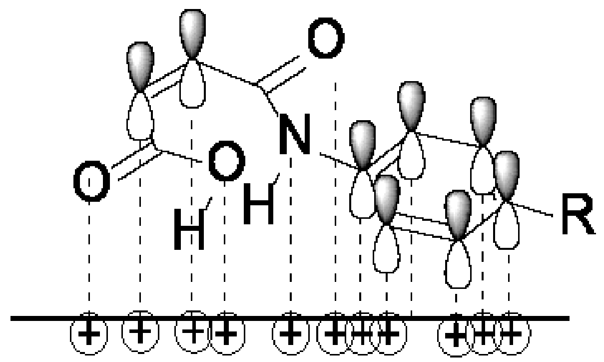

Figure 1: Adsorption of SOTB on the brass surface.

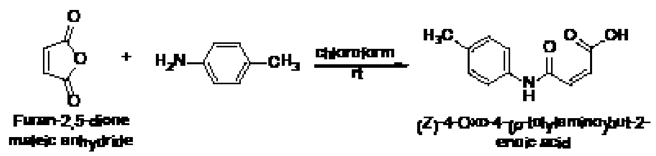

Figure 2: Synthesis of inhibitor.

Citation: El-Shamy AM, Elkarim MAA, Kalmouch A (2016) Mitigation of Sulfide Attach on α-Brass Surface by Using Sodium (Z)-4-Oxo-4-p-Tolyl-2-Butenoate. J Chem Eng Process Technol 7: 273. doi:10.4172/2157-7048.1000273

and anodic curves were obtained and depending on the inhibitor concentration. The maximum efficiency is observed at 250 ppm but by increasing the concentration the inhibition efficiency is decreased and it could be seed in Figure 4b which illustrates the effect of 250 and 300 ppm of inhibitor on the polarization curves. The results proved that the recommended dose is clearly identified at 250 ppm. These results are attributed with the agglomeration effect of organic inhibitor is existed at 300 ppm. The results proved that formation of a protective film from copper inhibitor complex, which is clearly seen from the appearing of a passive region at the anodic branch and the expected mechanism, is listed in Eq. 6 and 7. It is clearly noticed that the potential becomes more anodic reaches the break down potential, E_b, at the end of passive region. The current increases rapidly above E_b and at this point the localized corrosion is obtained as a result of the breakdown of the protective film [48]. The values of E_b were -0.079 and -0.048 V for blank and 250 ppm of SOTB respectively but in case of 300 ppm the value became -0.080 V, which also prove that the minimum effective dose is 250 ppm. It is also seen that the breakdown potential, E_b, is shifted to more positive potential and the values of current decreases which attributed with the formation of protective film on the brass surface. The corresponding electrochemical parameters are listed in Table 1 and we can notice that the corrosion potential values were shifted to more positive depending on the inhibitor concentration. The data proved that this inhibitor is mixed-type inhibitor because of controlling both cathodic and anodic reactions. Table 1 also mentions that the values of current density were decreased and the rate of decreasing is directly proportional with the inhibitor concentration. On the other hand the values of bc and ba proved that the inhibitor controlled both the cathodic and anodic reactions and the maximum inhibition efficiency is obtained at 250 ppm. The effect of sulfide ions on the polarization curve of brass in the SOTB inhibited solution is illustrated in Figure 5. The results show that the presence of sulfide ions makes moderately failure in the protective film and it is could be seen from the decreasing of breakdown potential values. The sulfide ion also affected on the current density values which increases it especially in the passive region and this indicates that the start of anodic dissolution. The values of open circuit potential become more negative by shifting it to the cathodic direction. Figure 6 presents the change of the corrosion rate and inhibition efficiency determined from polarization curves as a function of SOTB concentration. The inhibiting effect of the employed corrosion inhibitor is affected by its concentration; the increase of the SOTB increases the inhibition efficiency from 25 ppm to 250 ppm. As seen in Figure 6 the increase of concentration up to 250 ppm leads to decrease in the inhibition efficiency due to the agglomeration of organic compounds at certain concentration and this is clearly noticed from the increase of corrosion rate because of attacking the chloride ions.

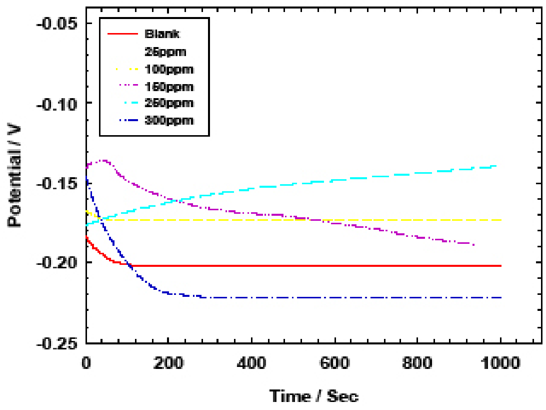

Figure 3: Open circuit potential curves of brass in 3.5% NaCl solution containing various concentrations of SOTB.

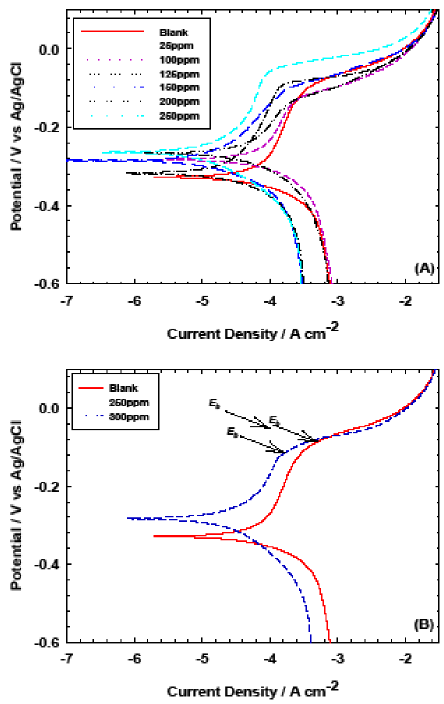

Figure 4: Polarization curves of brass in 3.5% NaCl solution (a) containing various concentrations of SOTB from 25 to 250 ppm (b) containing concentrations of 250 and 300 ppm from SOTB.

Electrochemical impedance spectroscopy (EIS) measurements

The effect of different concentration of inhibitor (25-200 ppm) on the corrosion behavior of brass in 3.5% NaCl solution has been studied by EIS measurements. Figure 7a shows the typical Nyquist impedance plot at an open-circuit potential value for brass without and with various concentration of SOTB. It is clearly seen that the brass electrode shows incomplete semicircle, denoting metals with protective oxide films [49]. The diameter of this semicircle increased with the increase of inhibitor concentration. This indicates that the existence and protection effect of adsorbed layer [50]. The data obtained from Nyquist plots were confirmed by plotting the values of impedance log IZI against log frequency for brass is illustrated in Figure 7b. The inhibited surface could be proved by the formation of highly resistive region in the area of high frequency and no plateau in low frequency and also the capacitive region is existed in the area of intermediate frequencies [51]. Figure 7b illustrates the Bode-phase formats (log f vs. Phase) from the plots it is obviously noticed that the maximum of the curve shift to low frequency with increasing maximum phase angle (60-80°C), which indicates inhibition of the corrosion process [52]. The inhibitive action of the corrosion inhibitor could be proved from the values of phase angle, which registered high values for inhibited solution if it compared with the solution without inhibitor. The best fitting for the equivalent circuit is formed from the plots analyzing model and the circuit is present in Figure 8 and the obtained impedance parameters from the equivalent circuit are recorded in Table 2. The R_S represents the solution resistance between brass electrodes and the SCE electrode, R_b and Cb are the resistance and capacitance of oxide layer,

Citation: El-Shamy AM, Elkarim MAA, Kalmouch A (2016) Mitigation of Sulfide Attach on α-Brass Surface by Using Sodium (Z)-4-Oxo-4-p-Tolyl-2-Butenoate. J Chem Eng Process Technol 7: 273. doi:10.4172/2157-7048.1000273

Inhibitor Conc., (ppm)	OCP (V) vs. SCE	E_{corr} (V) vs. SCE	b_a (V dec^{-1})	b_c (V dec^{-1})	I_{corr} (A cm^{-2})	C.R. mpy	I.E, (%)	R_p
Blank	-0.202	-0.3284	0.2126	0.4745	4.72e-4	5.89	------	354.89
25	-0.188	-0.2788	0.1974	0.4745	8.43e-5	1.05	82	784.15
100	-0.200	-0.2837	0.1003	0.2547	5.87e-5	0.73	88	532.67
150	-0.188	-0.2857	0.1248	0.2599	2.60e-5	0.33	94	1401.70
200	-0.223	-0.3180	0.2684	0.1208	2.78e-5	0.35	94	1406.30
250	-0.137	-0.2651	0.1524	0.2702	1.99e-5	0.24	96	2126.20
300	-0.222	-0.2830	0.2447	0.3020	5.75e-5	0.72	87	1020.50
0.01M Na_2S	-0.752	-0.4350	0.7544	1.3995	2.09e-4	2.6123	---	1018.50
250+HS^-	-0.198	-0.4342	0.2285	0.2999	3.30e-5	0.4124	84	1707.00

Table 1: Electrochemical parameters and inhibition efficiency for brass in 3.5% NaCl containing different concentrations of SOTB.

Inhibitor concentration ppm	Rs (ohm cm2)	Cb (uFcm-2)	Rb (ohm cm2)	Cp (uFcm-2)	Rp (ohm cm2)	I.E, (%)
Blank	9	11.8	173	41.5	1.3	-----
25	9.2	11.1	347	27	5.1	74.5
50	8.9	10.5	481	23.2	12.2	89.3
100	8.5	10.3	534	20.8	15.4	91.5
125	8.8	9.36	624	17.6	19.6	93.4
150	9.3	9.13	725	16.1	22.6	94.2
200	10	8.72	888	14.3	27	95.1
250	11.5	8.6	1130	13.5	29.9	96.6

Table 2: Electrochemical Impedance parameters and inhibition efficiency for brass in 3.5% NaCl containing different concentrations of SOTB.

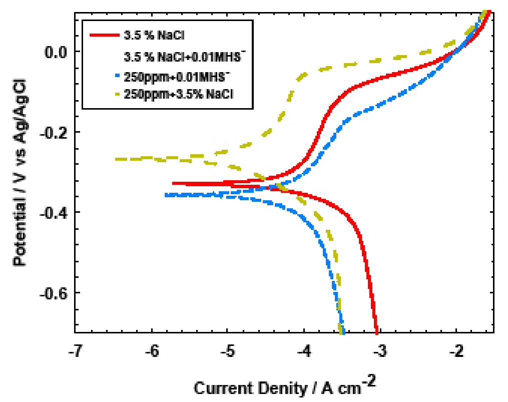

Figure 5: Effect of sulfide ions on the polarization curves of copper in the presence of 3.5% NaCl and/or 250 ppm of SOTB.

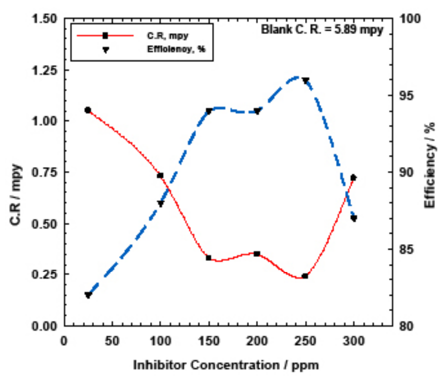

Figure 6: The change of the corrosion rate and inhibition efficiency determined from polarization curves as a function of SOTB concentration.

RP and C_p represents the resistance and capacitance of the protective film. The inhibition efficiency (IE%) was estimated from the values of Rp by using following equation [53].

$$IE\,(\%)=(R_{pinh}-R_p)/R_{pinh} \quad (14)$$

The protection of the brass surface against corrosion in the presence of inhibitor is attributed with the increasing of polarization resistance Rp (from 1300 ohm to 29900 ohm in presence of 25 ppm) [54]. The obtained data could be also proved by increasing in the thickness (d) of the double layer capacitor between the metal surface and the solution which is directly proportional to $1/C_p$, as it seen, the decreasing of value of capacitance from 41.5 to 13.5 $uFcm^{-2}$ (Table 2). The EIS data thus agree with the polarization data and both proved that SOTB is a good inhibitor for brass in unpolluted salt water solutions. Figure 9 represents the change of the impedance and capacitance determined from EIS curves as a function of SOTB concentration. The formed protective film resistance R_p determined from EIS curves is used to describe the inhibition efficiency of SOTB with regards to its concentrations. As seen from Figure 9 the R_p values are increased with the SOTB concentrations. These results prove that the thickness of the protective film is continuously increases to the maximum thickness at 250 ppm, which constitute the maximum inhibition efficiency. This behavior could be also proved from the determined capacitance C_p which decreases with concentration of inhibitor. Figure 10 shows the typical Nyquist impedance plot of brass in inhibited and uninhibited polluted sulfide salt water. The results proved that the stability of protective complexes is higher than that of Cu_2S so the inhibitor give inhibition efficiency of about 86% and is considered acceptable value specially if it compared with the efficiency of benzotriazole in sulfide media. The sulfide ions cause breakdown of the protective copper inhibitor complex so, the inhibitor shows moderate effect which is clearly noticed from SEM micrographs which illustrate missing parts from the protective film.

Surface characterization

Effect of chloride ions: The anti-corrosion influence of the employed corrosion inhibitor in unpolluted salt water is clearly showed in Figure 11a, the surface morphology of the brass electrode was investigated after immersion in 3.5% NaCl solutions and the image proved that the surface roughness is increased because of the presence of chloride ions. The dezincification process is clearly noticed and it is well know that the dissolution of zinc and copper is attributed with the chloride ions effect. Figure 11b illustrates the SEM micrographs of brass after immersion in inhibited 3.5% NaCl solutions with 250 ppm of SOTB. As seen in this micrograph the brass surface is covered with a very nice protective film from the corrosion inhibitor, and this film is formed

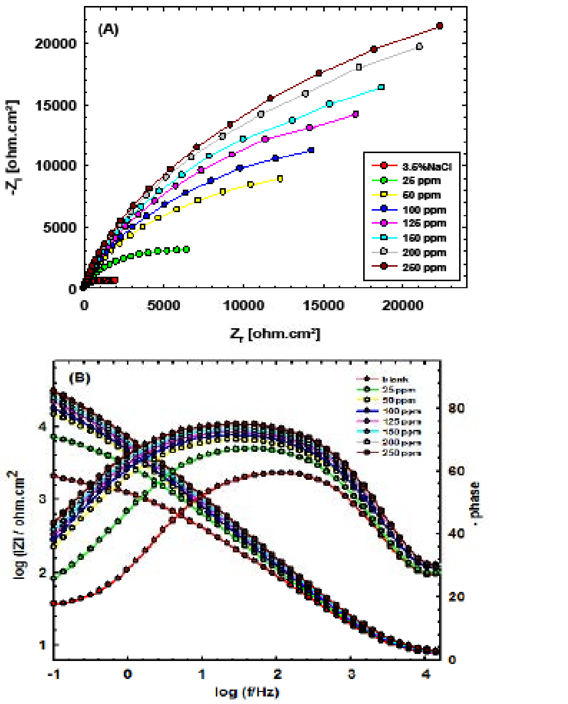

Figure 7: Electrochemical impedance spectra for brass in 3.5% NaCl containing various concentrations of SOTB (a) Nyquist plots (b) Bode plots and phase.

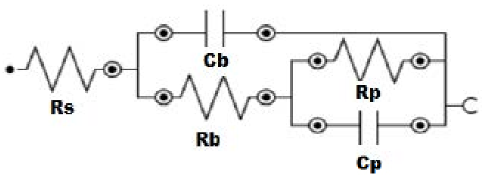

Figure 8: The equivalent circuit.

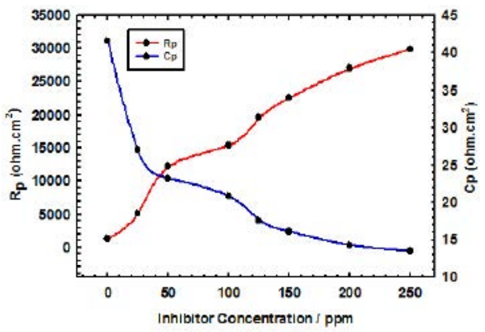

Figure 9: The change of the impedance and capacitance determined from EIS curves as a function of SOTB concentration.

from brass complex surface with a layer of Cu_2O which is extinguished to the protective layers. The obtained micrograph was subjected to EDS elemental analysis Figure 12a and Table 3 show that the highest content in chloride ions on the brass surface compared with the gained data from Figure 12b and Table 4. The EDS analysis revealed that the surface is enriched in copper (47.73%) with very low content of Zn (6.3%) which, indicating the occurrence of strong dezincification process but after using the inhibitor the EDS analysis revealed that the surface is lack in copper content (21.12%) with very low content of Zn (2.17%) which, indicating the decreasing of dezincification process and these results were agreed with the previous electrochemical measurements.

Effect of sulfide ions: Figure 13a and 13b show the effect of sulfide ions on the brass surface in absence and in the presence of inhibitor, respectively. The micrographs image proved that the sulfide ions have dangerous effect on the brass surface especially in absence of SOTB. On the other hand in the presence of SOTB the micrograph showed limited effect on the protective film and the surface roughness is decreased. The formed protective film from brass complex surface with a layer of Cu_2O is slightly affected by the sulfide attack. From the obtained data in Tables 5 and 6, the EDS analysis is revealed that the surface is contained high content in copper (49.79%) with very low content of Zn (8.12%) which, indicating the occurrence of strong dezincification process, this behavior is related to the effect of sulfide attach on brass surface. In the presence of SOTB the EDS analysis register lower content in copper (43.82%) with very low content of Zn (6.04%) which, indicating the SOTB decrease the effect of sulfide attack on the brass surface and reduce the dezincification process. The obtained results from surface characterization were completely agreed with the results of all electrochemical measurements (Figure 14).

Element	Weight %	Atomic %	Net Int.	Error %
C	16.38	38.61	13.54	16.79
O	6.95	12.29	19.14	15.98
Cl	16.87	13.47	237.95	4.43
Cu	47.73	21.26	161.29	3.75
Zn	6.3	2.73	17.42	15.79

Table 3: Elemental analysis of brass surface in unpolluted 3.5% NaCl.

Element	Weight %	Atomic %	Net Int.	Error %
C	52.99	74.73	72.58	11.3
N	5.77	11.65	4.87	28.76
O	13.33	14.11	29.71	13.86
Cl	10.38	4.96	168.45	3.57
Cu	21.12	5.63	71.8	5.24
Zn	2.17	0.56	6.04	28.48

Table 4: Elemental analysis of brass surface in 250 ppm of SOTB in unpolluted 3.5% NaCl.

Element	Weight %	Atomic %	Net Int.	Error %
O	11.77	28.4	46.45	12.1
Cl	24.03	26.16	363.44	4.4
Cu	49.79	30.25	187.71	3.58
Zn	8.12	4.8	25.05	14.1
Na	5.92	9.94	23.16	14.58
S	0.37	0.45	5.76	40.02

Table 5: Elemental analysis of brass surface in sulfide polluted 3.5% NaCl.

Element	Weight %	Atomic %	Net Int.	Error %
C	13.77	30.74	16.68	16.08
N	5.34	10.22	6.9	24.23
O	15.89	26.62	66.81	12
Cl	15.07	11.39	295	4.23
Cu	43.82	18.49	203.63	3.42
Zn	6.04	2.47	22.93	14.67
S	0.08	0.06	1.57	68.64

Table 6: Elemental analysis of brass surface in 250 ppm of SOTB in polluted 3.5% NaCl.

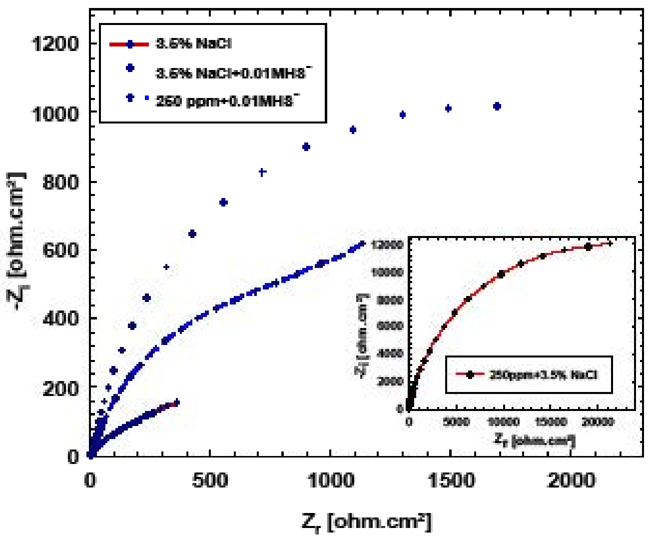

Figure 10: Nyquist plots of brass in 3.5% NaCl, 3.5% NaCl+250 ppm, 3.5% NaCl+0.01M HS^- and/or 3.5% NaCl+250 ppm+0.01M HS^-.

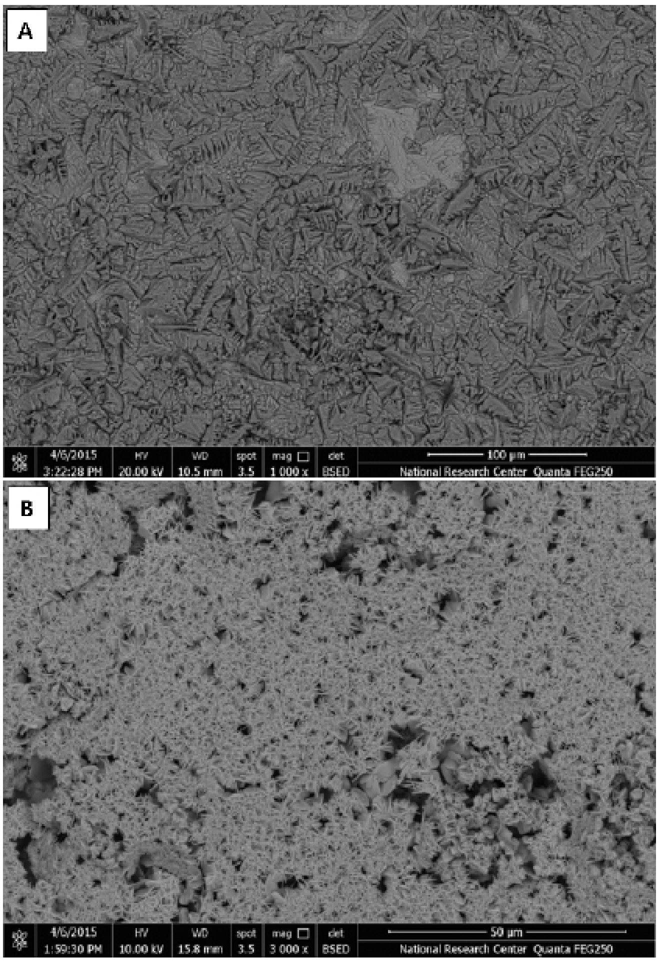

Figure 11: SEM micrographs of brass after immersion in 3.5% NaCl solutions in (a) absence of SOTB and (b) presence of 250 ppm of SOTB.

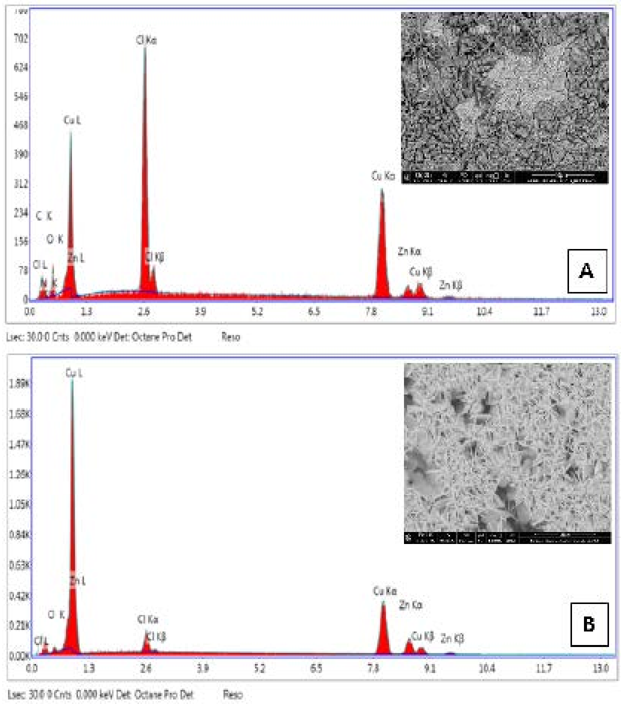

Figure 12: EDS of brass in (a) 3.5% NaCl and (b) 3.5% NaCl+250 ppm of SOTB.

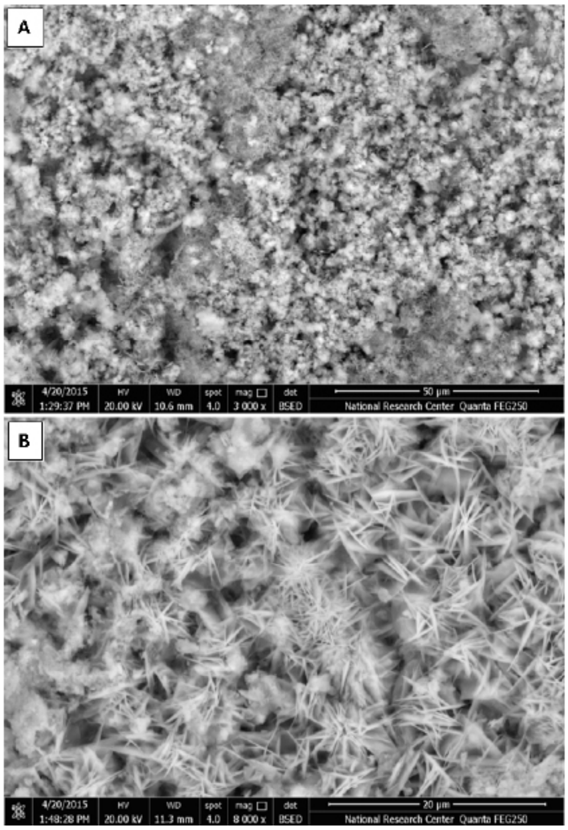

Figure 13: SEM micrographs of brass after immersion in 3.5% NaCl+0.01M HS^- solutions in (a) absence of SOTB and (b) presence of 250 ppm of SOTB.

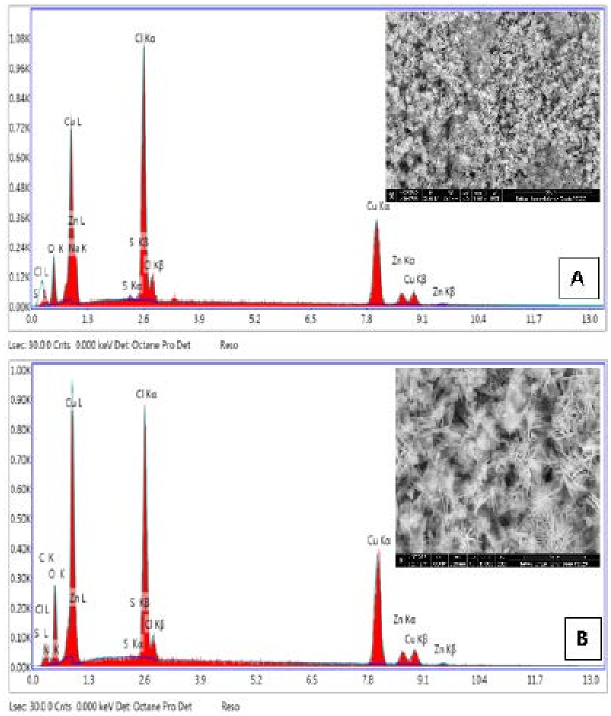

Figure 14: EDS of brass in (a) 3.5% NaCl+0.01M HS^- and (b) 3.5% NaCl+0.01M HS^-+250 ppm of SOTB.

Conclusions

The SOTB is considered a very good inhibitor for brass in unpolluted and polluted salt water. The recommended dose of SOTB is 250 ppm in unpolluted salt water with efficiency of 96%. The corrosion inhibitor is act as anodic and cathodic inhibitor with high stability for the protected film due to the stability of the brass inhibitor complex. The chloride ions have highly effect on the brass surface through the dissolution of copper and zinc through the dezincification process and this process is decreased in the presence of SOTB by forming very stable adsorbed layers on the brass surface. The adsorbed layers is slightly affected by the sulfide ions and this results of SOTB are considered as an excellent results if it compared with the benzotriazole if it affected by sulfide ions. As seen from Table 1 the inhibition efficiency of SOTB in polluted sulfide salt water is about 84% which register 12.5% decreasing in the inhibition efficiency in unpolluted media. The decrease in the inhibition efficiency is related to the moderate sulfide attack on the protective film, the SEM and EDS proved that the sulfide attack has very low effect on SOTB brass complex. The SOTB corrosion inhibitor is could be used in application as a very good inhibitor in unpolluted and sulfide polluted salt water.

References

1. Dinnappa RK, Mayanna SM (1987) Corr Sci 27: 349-361.
2. El-Sayed MS, El-Shamy AM, Mostafa MR, Ahmed OHE (2007) 5-(Phenyl)-4H-1,2,4-triazole-3-thiol as a corrosion inhibitor for copper in 3.5% NaCl solutions. Material Chemistry and Physics 102: 231-239.
3. Newman RC, Shahrabi T, Sieradzki K (1988) Direct electrochemical measurement of dezincification including the effect of alloyed arsenic. Corr Sci 28: 873-879.
4. Alkhrafi FM, El-Shamy AM, Ateya BG (2009) Effect of 3-aminotriazole on the Corrosion of Copper in Polluted and Unpolluted Media. J Chem and Chemic Eng 3: 42-50, 56.
5. Trethewey R, Pinwill I (1987) Surf and Coat Tech 30: 289-307.
6. Alkhrafi FM, El-Shamy AM, Ateya BG (2009) Comparative Effects of Tolytriazole and Benzotriazole Against Sulfide Attack on Copper. Int J Electrochem Sci 4: 1351-1364.
7. Joseph G, Arce MT (1967) Corr Sci 7: 597-605.
8. El-Shamy M, Samir TG, El Meleigy AE (2013) Int J of Rec Devel Eng and Tech 1: 11-18.
9. Pchelnikov P, Sitnikov AD, Marshakov IK, Losev VV (1981) A study of the kinetics and mechanism of brass dezincification by radiotracer and electrochemical methods. Electrochimica Acta 26: 591-600.
10. Polunin V, Pchelnikov AP, Losev VV, Marshakov IK (1982) Electrochemical studies of the kinetics and mechanism of brass dezincification. Electrochimica Acta 27: 467-475.
11. El-Shamy M, Shehata MF, Samir TG, Eman AE (2015) Journal of Advances in Chemistry 11: 3441-3451.
12. El-Shamy M, Zohdy KM (2015) Journal of Applied Chemical Science International 2: 56-64.
13. El-Sayed MS, Adel TA, Gopi D, El-Shamy AM (2014) Corrosion and Corrosion Inhibition of High Strength Low Alloy Steel in 2.0 M Sulfuric Acid Solutions by 3-Amino-1,2,3-triazole as a Corrosion Inhibitor. Journal of Chemistry. Article ID 538794, pp: 1-8.
14. El-Sayed MS, Adel TA, Halfa H, El-Shamy AM (2015) Corrosion of High Strength Steel in Concentrated Sulfuric Acid Pickling Solutions and Its Inhibition by 3-Amino-5-mercapto-1,2,3-triazole. Int J Electrochem Sci 10: 1777-1791.
15. Javaherdashti R, Nwaoha C, Tan H (2013) Corrosion and materials in the oil and gas industries, CRC Press. Taylor & Francis Group. Chapter 19. Cathodic Protection in the Oil and Gas Industry. pp: 489-510.
16. Neelam G, Abhinav A (2014) Microbes in Process. NOVA Science Publishers. Chapter 14. El-Shamy AM. Control of Corrosion Caused by Sulfate-Reducing Bacteria. pp: 337-362.
17. El Taib HF, Haruyama S (1980) Corrosion Sci 20: 887.
18. Mansikkamaki K, Johans CK (2006) Electrochem Soc 153: 22.
19. Cao PG, Yao JL, Zheng JW, Gu RA, Tian ZQ (2002) Comparative Study of Inhibition Effects of Benzotriazole for Metals in Neutral Solutions as Observed with Surface-Enhanced Raman Spectroscopy. Langmuir 18: 100-104.
20. Metikos-Hukovic M, Babic R, Marinovic A (1998) Spectrochemical Characterization of Benzotriazole on Copper. J Electrochem Soc 145: 4045-4051.
21. Ho Yeung H, Chan G, Weaver MJ (1999) A Vibrational Structural Analysis of Benzotriazole Adsorption and Phase Film Formation on Copper Using Surface-Enhanced Raman Spectroscopy. Langmuir 15: 3348-3355.
22. Polewska W, Vogt MR, Magnussen OM, Behm RJ (1999) In Situ STM Study of Cu(111) Surface Structure and Corrosion in Pure and Benzotriazole-Containing Sulfuric Acid Solution. J Phys Chem B 103: 10440-10451.
23. Youda R, Nishihara H, Aramaki K (1990) Sers and impedance study of the equilibrium between complex formation and adsorption of benzotriazole and 4-hydroxybenzotriazole on a copper electrode in sulphate solutions. Electrochem Acta 35: 1011-1017.
24. Jin-Hua L, Zhi-Cheng C, Shu N, Li-Hua H, Shou-Zhuo Y (1998) An XPS and BAW sensor study of the structure and real-time growth behaviour of a complex surface film on copper in sodium chloride solutions (pH = 9), containing a low concentration of benzotriazole. Electrochim Acta 43: 265-274.
25. Schultz ZD, Biggin ME, White JO, Gewirth AA (2004) Infrared−Visible Sum Frequency Generation Investigation of Cu Corrosion Inhibition with Benzotriazole. Analytical Chemistry 76: 604-609.
26. Xu Z, Lau S, Bohn PW (1993) The role of benzotriazole in corrosion inhibition: formation of an oriented monolayer on Cu2O. Surf Sci 296: 57-66.
27. Qafsaoui W, Blanc C, Pebere N, Takenouti H, Srhiri A, et al. (2002) Quantitative characterization of protective films grown on copper in the presence of different triazole derivative inhibitors. Electrochim Acta 47: 4339-4346.
28. Frignani A, Fonsati M, Monticelli C, Brunoro G (1999) Influence of the alkyl chain on the protective effects of 1,2,3-benzotriazole towards copper corrosion. Part ii: formation and characterization of the protective films. Corros Sci 41: 1217-1227.

29. Jiang Y, Adams JB, Sun D (2004) Benzotriazole Adsorption on Cu2O(111) Surfaces: A First-Principles Study. J Phys Chem 108: 12851-12857.

30. Zucchi F, Trabanelli G, Monticelli C (1996) The inhibition of copper corrosion in 0.1 M NaCl under heat exchange conditions. Corrosion Sci 38: 147-154.

31. Zucchi F, Trabanelli G, Fonsati M (1996) Tetrazole derivatives as corrosion inhibitors for copper in chloride solutions. Corrosion Sci 38: 2019-2029.

32. Tommesani L, Brunoro G, Frignani A, Monticelli C, Dal Colle M (1997) On the protective action of 1,2,3-benzotriazole derivative films against copper corrosion. Corrosion Sci 37: 1221-1237.

33. Da-quan Z, Li-xin G, Guo-ding Z (2004) Inhibition of copper corrosion in aerated hydrochloric acid solution by heterocyclic compounds containing a mercapto group. Corrosion Sci 46: 3031-3040.

34. Macdonald D, Syrett BC, Wing SS (1979) The Corrosion of Cu-Ni Alloys 706 and 715 in Flowing Sea Water. II – Effect of Dissolved Sulfide. Corrosion 35: 367-378.

35. Gudas JP, Hack HP (1979) Sulfide induced corrosion of copper nickel alloys. Corrosion 35: 67-73.

36. de Sanchez SR, Schiffrin DJ (1982) Corros Sci 22: 85.

37. Kato C, Pickering HW, Castle JE (1984) Effect of Sulfide on the Corrosion of Cu-9.4 Ni-1.7 Fe Alloy in Aqueous NaCl Solution. J Electrochem Soc 131: 1225-1229.

38. Alhajji JN, Reda MR (1994) The Conflicting Roles of Complexing Agents on the Corrosion of Copper-Nickel Alloys in Sulfide Polluted Seawater. J Electrochem Soc 141: 1432-1439.

39. Smith J, Qin Z, King F, Werme L, Shoesmith DW (2007) Sulfide Film Formation on Copper under Electrochemical and Natural Corrosion Conditions. Corrosion 63: 135-144.

40. Andricopulo D, Yunes RA, Filho VC, Nunes RJ (1999) Development of a predictive statistical model for the analgesic activity of a family of imides. Pharmazi 54: 698-704.

41. Lopez SN, Sortino M, Escalante A (2003) Arzneim- Forsch /Drugs Res 53: 280.

42. Lima EQ, Queiroz EF, Andricopulo AD, Nunes JR, Yunes RA (1999) Bol Soc Chil Quim 44: 185.

43. Indap MA, Ambaye RY (1991) Efficacy of 5-fluorouracil in combination with methoxyphenyl maleamic acid in murine tumors. J Postgrad Med 37: 211-215.

44. Osamu K, Baruch R, John EC (1985) N-Phenyl-maleimides, -isomaleimides and - maleamic Acids as Selective Herbicide Antidotes. Agric Bioi Chem 49: 267-268.

45. Tamas KI, Kriton KH (1991) Chemistry and Structure-Activity Relationships of Herbicide Safeners. Z Naturforsch 46: 798-804.

46. Abdullah M, Al-kharafi FM, Ateya BG (2006) Intergranular corrosion of copper in the presence of benzotriazole. Scripta Materilaia 54: 1673-1677.

47. Ateya AG, Al-Kharafi FM, Al-Azab AS (2003) Electrodeposition of Sulfur from Sulfide Contaminated Brines. Electrochem Solid St 6: C137-140.

48. Stern M, Geary AL (1957) Electrochemical Polarization I. A Theoretical Analysis of the Shape of Polarization Curves. J Electrochem Soc 104: 56-63.

49. Cottis R, Turgoose S (1999) Electrochemical Impedance and Noise. NACE International, Texas, USA.

50. Ma H, Chen S, Niu L, Zhao S, Li S, et al. (2002) Inhibition of copper corrosion by several Schiff bases in aerated halide solutions. J Appl Electrochem 32: 65-72.

51. Ismail KM, El-Moneim AA, Badawy WA (2001) Stability of Sputter-Deposited Amorphous Mn-Ta Alloys in Chloride-Free and Chloride- containing H_2SO_4 Solutions. J Electrochem Soc 148: 81-87.

52. Sherif EM, Erasmus RM, Comins JD (2008) Inhibition of copper corrosion in acidic chloride pickling solutions by 5-(3-aminophenyl)-tetrazole as a corrosion inhibitor. Corros Sci 50 3439-3445.

53. Quraishi MA, Sardar R (2003) Hector bases - a new class of heterocyclic corrosion inhibitors for mild steel in acid solutions. J Appl Electrochem 33: 1163-1168.

54. Mansfeld, Lin S, Kim S, Shih H (1987) Pitting and surface modification of SIC/ Al. Corros Sci 27: 997-1000.